ACS OMEGA

Open Access

http://pubs.acs.org/journal/acsodf

Article

Upgrading Pyrolysis Bio-Oil through Esterification Process and Assessing the Performance and Emissions of Diesel−Biodiesel−Esterified Pyrolysis Bio-Oil Blends in Direct Injection Diesel Engines

Sutthichai Khamhuatoey, Sommas Kaewluan, Jarernporn Thawornprasert, Ye Min Oo, Kritsakon Pongraktham, and Krit Somnuk*

Cite This: *ACS Omega* 2023, 8, 44586−44600

Read Online

ACCESS | Metrics & More | Article Recommendations

ABSTRACT: This research aimed to evaluate the performance and emissions of direct injection diesel engines using blends of diesel−biodiesel−esterified pyrolysis bio-oil (D−B−EPB). The pyrolysis process was employed to produce pyrolysis bio-oil (PBO) from solid biomass obtained from fresh palm fruits. Furthermore, a simple and effective esterification process was used to upgrade the PBO. The methyl ester (ME) purity of EPB production was studied to optimize three independent variables: methanol (14.8−65.2 wt %), sulfuric acid (1.6−18.4 wt %), and reaction time (16−84 min) using the response surface methodology. The actual experiment yielded a ME purity of 72.73 wt % under the recommended conditions of 40.3 wt % methanol, 13.0 wt % sulfuric acid, 50 min reaction time, 60 °C reaction temperature, and 300 rpm stirrer speed. Additionally, the stability and phase behaviors of D−B−EPB blends were analyzed by using a ternary phase diagram to determine the potential blending proportion. The results revealed that a fuel blend consisting of 30 wt % diesel, 60 wt % biodiesel, and 10 wt % EPB (D30B60EPB10) met the density and viscosity requirements of diesel standards. This D30B60EPB10 blend was subjected to performance and emission tests in diesel engines at various speeds ranging from 1100 to 2300 rpm and different engine loads of 25, 50, and 75%. In terms of performance analysis, the brake thermal efficiencies of biodiesel and D30B60EPB10 were 7.19 and 3.88% higher than that of diesel, respectively. However, the brake-specific fuel consumption of the D30B60EPB10 blend was 6.60% higher than that of diesel due to its higher density and viscosity and lower heating value compared with that of diesel. In the emission analysis, the D30B60EPB10 blend exhibited performance comparable to diesel while being more environmentally friendly, reducing carbon monoxide, carbon dioxide, nitrogen oxide, and smoke opacity by 8.73, 30.13, 37.55, and 59.75%, respectively. The results of this study suggest that the D−B−EPB blend has the potential to serve as a viable biofuel option, reducing the proportion of diesel in blended fuel and benefiting farmers and rural communities..

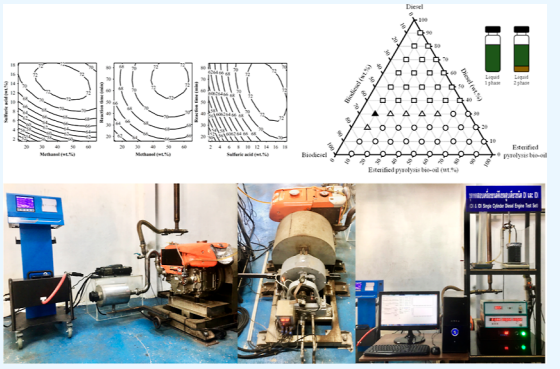

1. INTRODUCTION

The widespread adoption of fossil fuels as the primary energy source has resulted in severe shortages in certain sectors today. As a result, industrial sectors have transitioned from using petroleum fuel to biomass fuel in order to reduce production costs and minimize plant waste. There is a growing interest in utilizing biomass resources to generate fuels and chemical feedstocks, which are considered promising renewable energy sources.[1,2] Biomass can be sourced in several ways: (i) after the harvesting of crops such as stalks, rice straw, sugar cane, cassava leaves, and shoots; (ii) through the processing of agricultural crops such as bagasse, rice husk, corn cob, sawdust, slab palm fiber, and palm, among others; and (iii) from biogenic components found in domestic rubbish such as food, wool products, cotton, paper, yard, and wood wastes.[2,3] These biomasses can be transformed into usable energy through various methods, including (i) direct burning (combustion to obtain heat); (ii) thermochemical processes to convert solid, gaseous, and liquid fuels; (iii) chemical conversion processes to generate liquid fuels; and (iv) biological conversion processes to produce liquid and gaseous fuels.[3] There is significant potential for developing the use of biomass liquid fuel as an alternative fuel for compression ignition (CI) engines,

Received: July 12, 2023
Revised: October 24, 2023
Accepted: October 31, 2023
Published: November 13, 2023

particularly in agriculture-dependent and developing countries.[4] Biochemical and thermochemical conversion methods are commonly employed to unlock the energy potential of biomass. Biochemical conversion techniques rely on biological activity to convert biomass into alcohol or oxygenated molecules.[5] Thermochemical processes, such as pyrolysis, liquefaction, gasification, and supercritical fluid extraction, are also used.[6] Among these processes, pyrolysis stands out due to its high conversion efficiency, independence from external feedstock, and low-pressure operation. Pyrolysis is considered one of the most promising thermochemical conversion processes for agricultural crop residues with low energy density, producing pyrolysis bio-oil (PBO).[7,8]

When comparing biomass raw materials, PBO is a renewable energy source that has the potential to reduce dependence on nonrenewable fossil fuels.[9] Despite the increasing importance of electric vehicles, there is still a significant demand for CI engines. The use of PBO in a diesel engine has been found to enhance combustion efficiency and reduce CO, CO_2, and NO_x emissions. Pandey et al.[10] conducted a study on the performance and emission analysis of PBO blends with diesel (PBO 5, 10, 15, 20, 25, and 30%) in a CI engine. At maximum load, the 30% PBO blend exhibited the lowest CO and CO_2 emissions among all the blends due to the abundant availability of oxygen within the combustion chamber. The presence of oxygen in the bio-oil facilitates the conversion of CO to CO_2 during the combustion process, resulting in a leaner mixture. These fuels are classified as carbon-neutral fuels due to their beneficial impact on reducing carbon emissions.[10] In terms of raw materials for biomass and biofuel production, palm oil is recognized as one of the largest sources for the production of biodiesel, biomass, and bio-oil. It is a rapidly developing low-cost tropical plant species.[11]

In the global market, Indonesia and Malaysia, the two main palm oil producers, have significant influence on palm oil pricing. Malaysia produces 19.7 million tons of palm oil annually, while Indonesia produces 39.5 million tons. Although Thailand is the third-largest palm oil producer globally, its contribution to the market accounts for only 3.9% of the total production. Palm oil yields per unit of land are 6−10 times higher compared with soy, rapeseed, sunflower, coconut, and olive oil yields.[12] Consequently, among all vegetable oils, palm oil has the lowest production cost. Palm oil plantations play a crucial role in Malaysia, providing substantial funds and employment opportunities for numerous rural communities.[13] When overstock of palm oil rose in the world's leading palm oil producers of Indonesia, Malaysia, and Thailand, those governments adopted strategies for coping with the situation and helped palm farmers in each of their countries. Another reason for the highest blend of palm oil in these countries is to reduce reliance on imported diesel. In Indonesia, the government is planning to promote the mandatory biodiesel with 35% palm oil content (B35) from B30. The Indonesia's economic ministry is convinced that this promotion will not affect the domestic cooking availability and food industry. Because the government requests and promotes local cooking oil production in domestic market as well to meet rising demand, this will help to support regular incomes of the labor in the agricultural sector.[14] Moreover, the boosting of using palm oil in Indonesia targets the requirements of energy security and renewable energy supply by 2025.[15] In Malaysia, the B20 biodiesel program was introduced in January 2020, with gradual implementation planned at the end of 2022. Malaysia has a plan to start a biodiesel program with 40% blending (B40) in the transport sector. However, the government committed that this biodiesel program was postponed due to the pandemic-related delay.[16] In Thailand, diesel B10 replaced diesel B7 since January 2020, after being designated as the standard diesel by the Ministry of Energy, Thailand. Moreover, the ministry has encouraged diesel B20 to be used by heavy trucks and buses to promote the steady raising of the proportion of biodiesel in the diesel mixing.[17] Thailand produced approximately 2.96 million tons of crude palm oil (CPO) in 2021, and 1.15 million tons of CPO were applied to the biodiesel production sector. In Thailand, the 48% of CPO goes to the biodiesel production sector and 52% of CPO was applied for the domestic cooking and food industry.[18] Thailand government concerns and balances the CPO production on both biodiesel production and food security issue. Typically, palm fruit can be utilized as a source of renewable energy to produce biodiesel from CPO obtained through the palm mill extraction processes. Furthermore, when appropriate processes such as pyrolysis are applied, palm fruit can become a viable source of renewable energy. Much of the research has focused on the production of PBO from solid biomass byproducts of palm oil mill plants. For instance, Sukiran et al.,[19] Salema and Ani,[20] and Sembiring et al.[21] employed empty palm fruit brunch as a raw material to produce PBO. Other researchers such as Salema and Ani,[22] Abnisa et al.,[23] and Mushtaq et al.[24] used palm shells for pyrolysis-based bio-oil production. However, no previous studies have explored the utilization of palm fruit as a solid biomass source for pyrolysis-based bio-oil production. Therefore, this research aims to investigate the feasibility of converting fresh palm fruits into liquid fuel, which is one of the objectives of the study's objectives.

During the pyrolysis process, palm fruits undergo various stages of thermal breakdown in an oxygen-depleted environment. Consequently, liquid, carbon-rich solid residue and gaseous fuels are produced simultaneously. However, when PBO was directly blended with diesel, it either rapidly separated into phases or was not resistant to the emulsion phase. This is due to the low miscibility, variable surface tension, and hygroscopic properties of these heavy oils.[25] Typically, bio-oils have acid values ranging from 7 to 12% (acid number of 50−100 mg KOH/g) and a pH of 2−4, which leads to reduced yields and increased corrosion rates with higher water content in PBO.[26] Fu et al.[27] stated that PBO chemical compositions consist of complex acids, aldehydes, ketones, esters, alcohols, phenols, and water, which must be eliminated through esterification to reduce viscosity and increase pH. Thus, the esterification process is necessary to decrease acid values, viscosity, density, and ash content in PBO. Alcohol and acid catalysts can be employed in the esterification process to enhance bio-oil characteristics.[27] The esterification process effectively reduces the acidity and viscosity of PBO by converting acetic acid to ethyl acetate.[28]

Emulsifying bio-oil with diesel is considered one of the most practical and efficient methods to enhance the use of bio-oil as a power fuel in internal combustion engines.[25] The emulsification of bio-oil and biodiesel presents potential as an alternative fuel to traditional power fuels due to their favorable combustion and emission characteristics, which can lead to lower fuel consumption and pollutant emissions.[27] According to several studies conducted by Ikura et al.,[29] Chiaramonti et al.,[30] Lin et al.,[31] and Martin et al.,[32] wood

https://doi.org/10.1021/acsomega.3c05007
ACS Omega 2023, 8, 44586−44600

Table 1. Fuel Characteristics of Diesel, Biodiesel, EPB, and D30B60EPB10 Blend

property	diesel standard	diesel (B10)	biodiesel	EPB	D30B60EPB10[c]
density at 15 °C (kg/m^3)	810−870	828	877	892	864
viscosity at 40 °C (cSt)	1.8−4.1	2.95	4.46[b]	6.94	4.07
cloud point (°C)		0	13		6
pour point (°C)	<10[a]	−9	12	4	4
acid value (mgKOH/g)		0.24	0.28[b]	3.09	0.55
copper strip corrosion	<no.1[a]	<no.1[a]	no.1a[b]	no.1a	no.1a
higher heating value (MJ/kg)		46.4	39.6	42.4	41.9
LHV (MJ/kg)		43.3	36.8	39.8	39.1
ME		9−10 vol %[a]	99.31 wt %	72.73 wt %	69.32 wt %
methanol (wt %)			<0.01[b]	3.31	

[a]Ministry of energy.[38] [b]Somnuk et al.[37] [c]D30B60EPB10 blend consisted of 30 wt % diesel + 60 wt % biodiesel + 10 wt % EPB.

biomass is the most commonly used raw material for producing PBO, which can then be used to create bio-oil emulsions with diesel. However, the potential of PBO derived from wood biomass is limited due to slow growth and restricted production capacity resulting from environmental regulations and policies. Conversely, agricultural crop residues serve as a viable alternative source of PBO for bio-oil in diesel production and offer several benefits over other sources, including high PBO yield, short growing cycles, and abundant readily available resources. Moreover, the utilization of PBO derived from agricultural crop residues has the potential to reduce the consumption of fossil diesel fuel in the production of this emulsion fuel, serving as an alternative for diesel engines. Furthermore, PBO has shown promise in reducing exhaust pollutant emissions compared with the use of diesel fuel.[27] Paramasivam et al.[33] studied the properties of bio-oil produced from the pyrolysis process of *Aegle marmelos* (AM) seed cake. Three blending percentages of 10, 15, and 20% bio-oil mixed with diesel were tested in a diesel engine. For HC emissions, 20% bio-oil emitted more HC than diesel fuel under all engine load conditions. At the highest load, the maximum NO_x emissions of 10, 15, and 20% bio-oil and diesel emitted 1437, 1498, 1501, and 1511 ppm, respectively. In terms of CO emissions, bio-oil blends significantly reduced CO levels compared to diesel fuel. Diesel exhibited the highest CO value emissions under all loading conditions compared to all other test fuels. At maximum load, 10, 15, and 20% bio-oil and diesel generated CO emissions of 0.53, 0.29, 0.17, and 0.74%, respectively. It showed that the highest bio-oil blend emitted the lowest CO emission. Therefore, as compared to diesel fuel, bio-oil from AM produced through pyrolysis tests emitted less NO_x and CO emissions. In the research of Sukumar et al.,[34] bio-oil derived from the pyrolysis of sweet lime empty fruit bunch was used as fuel in diesel engine. Various blend ratios of B20BOSL-J 5%, B20BOSL-J 10%, B20BOSL-J 15%, and B20BOSL-J 20% were utilized to analyze the emission and performance of the diesel engine. Their results showed that the lower NO_x emission was found in the BOSL-J blend when compared to the diesel. Moreover, the exhaust gas temperature (EGT) of bio-oil fuel blends was lower than that of diesel because the duration of the delay was affected by the usage of bio-oil blends, with shorter delay durations resulting in delayed combustion and decreased EGT. At the maximum load, the EGTs of 5, 10, 15, and 20% of BOSL-J blend and diesel were approximately 370, 340, 330, 320, and 380 °C, respectively.

The primary objective of this work was to investigate the conversion of solid biomass (palm fruits) into PBO (a liquid biofuel) through a pyrolysis process, followed by the upgrading of PBO using a simple and effective esterification process. The utilization of esterification offered advantages over fractional distillation including lower operating temperatures, reduced pumping power requirements, and simplified installation and maintenance procedures for achieving high-grade liquid fuel. Additionally, this study focused on using palm fruit as a raw material to produce PBO, whereas most research utilized empty palm fruit bunches and palm shells. The expectation was that PBO derived from palm fruit would possess superior physical properties, such as density, viscosity, pH, and high heating value, resulting in the production of high-grade liquid fuel. For an example of physical properties, PBO from empty palm fruit branches and palm shells had densities of 1032 and 1051 kg/m^3 and viscosities of 1.7 and 3.2 cP, respectively,[35,36] while the density and viscosity of PBO from palm fruit in our investigation were 863 kg/m^3 and 7.0 cP, respectively. The esterification process for upgrading PBO and various parameters such as methanol, sulfuric acid, and reaction time were optimized by using a response surface methodology (RSM). Upgrading PBO using the esterification process increases the purity of methyl ester (ME). It helps reduce acidity, increase the purity of ME, and improve fuel properties such as the density, viscosity, and calorific value. However, no previous studies have explored the utilization of palm fruit as a solid biomass source for pyrolysis-based bio-oil production. Therefore, this research aims to investigate the feasibility of converting fresh palm fruits into liquid fuel, which is one of the study's objectives. This work includes studying the purity of MEs from bio-oil upgraded by the esterification process, which differs from other studies. Usually, palm fruit is the raw material extracted as CPO for use in the food and biodiesel industries. During the oversupply of palm fruit in Thailand, palm fruit is used through a pyrolysis process without an extraction process, which is a simple process and helps farmers in one way. The second objective was to investigate the impact of emulsifying upgraded PBO with diesel and biodiesel and studying the influence of the fuel properties for its use as an alternative fuel in a diesel engine. The stability and phase behaviors of diesel−biodiesel−esterified pyrolysis bio-oil (D−B−EPB) blends were analyzed by using a ternary phase diagram. To the best of the authors' knowledge, the stability and fuel properties of D−B−EPB blends in varying proportions have not been previously investigated. Finally, an unmodified direct injection diesel [brake power (P_b), brake-specific fuel consumption (BSFC), and brake thermal efficiency (BTE)] and emissions (O_2, CO, CO_2, NO_x, EGT, and smoke opacity) of diesel, biodiesel, and a D−B−EPB

https://doi.org/10.1021/acsomega.3c05007
ACS Omega 2023, 8, 44586−44600

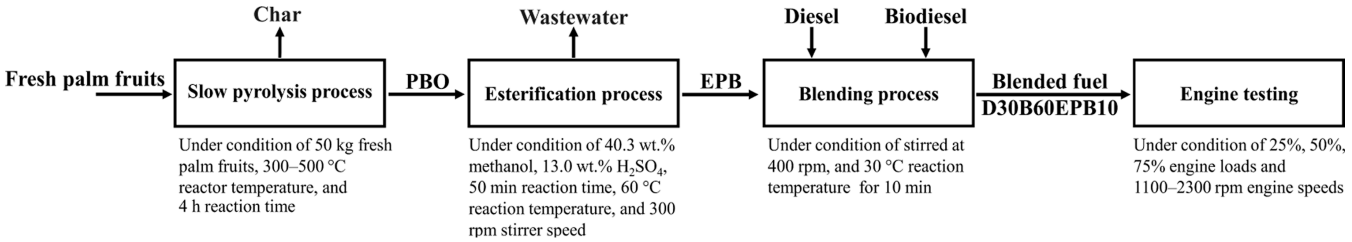

Figure 1. Schematic diagram of the slow pyrolysis process, esterification process, blending process, and engine testing.

blend at speeds of 1100, 1400, 1700, 2000, and 2300 rpm with 25, 50, and 75% engine load.

2. MATERIALS AND METHODS

2.1. Materials. The phase stability of D−B−EPB was investigated by using diesel B10 (10% ME with 90% diesel) obtained from a gas station. CPO with a high free fatty acid (FFA) content was purchased from a palm oil mill in southern Thailand. The properties of the CPO are as follows: a density of 0.916 kg/L at 60 °C, a viscosity of 18.17 cP at 60 °C, 13.699 wt % FFA, 83.116 wt % triglyceride, 2.882 wt % diglyceride, 0.244 wt % monoglyceride, 0.059 wt % ester, 0.312% water content, and an acid value of 30.0 mgKOH/g. Biodiesel (B100) was produced from the CPO using a two-step circulation process through the bundle tubes of the static mixer reactor, which consisted of two bundle tubes of the static mixer.[37] Thus, B100 derived from CPO was used as a component in the fuel blends to examine the phase stability and test it in a diesel engine. The properties of B100 are presented in Table 1.

In the PBO production process, the oil was extracted through slow pyrolysis from palm fruits under the conditions of 50 kg of palm fruits, a reactor temperature ranging from 300 to 500 °C, and a reaction time of 4 h. The properties of the PBO are as follows: a density of 0.863 kg/L at 30 °C, a viscosity of 8.20 cSt at 40 °C, a lower heating value (LHV) of 38.78 MJ/kg, an acid value of 101.36 mgKOH/g, a water content of 0.414 wt %, and a ME content of 3.37 wt %. The physical properties of the PBO were enhanced by employing the acid-catalyzed esterification process to convert the high FFA content of the CPO into ME, as described in eq 1. The final product of the esterification process, known as EPB, was used as a component in the fuel blends. The entire process of slow pyrolysis from palm fruits and the upgrading of PBO through esterification are illustrated in Figure 1. The experiments on the esterification process utilized purely commercial-grade chemicals, including 99% methanol and 98% sulfuric acid. The details of upgrading PBO using the esterification process are described in the next section. The properties of diesel, biodiesel, and EPB are listed in Table 1.

$$\text{FFA} + \text{Methanol} \overset{H_2SO_4}{\longleftrightarrow} \text{Methyl ester} + \text{Water} \quad (1)$$

2.2. Upgrading Pyrolysis Bio-Oil by the Esterification Process. *2.2.1. Experimental Design.* To assess the effectiveness of the design of experiments and optimize ME production from PBO, a central composite design (CCD) was employed in conjunction with RSM. The goal was to identify the optimal conditions for investigating ME purity in EPB. The RSM utilized a three-factor and five-level CCD, where experimental designs varied within the ranges of methanol content (14.8−65.2 wt %), sulfuric acid content (1.6−18.4 wt %), and reaction time (16−84 min), represented by the levels −1.682, −1, 0, +1, and +1.682. Table 2 presents the variables and their corresponding code levels, whereas Table 3 shows the experimental design encompassing 18 experiments. The purities of ME were analyzed using second-order polynomial equations and multiple regression analysis, as shown in eq 2.

Table 2. Independent Variables and Code Levels of RSM Experiments

		coded variable level				
independent variables	units	−1.682	−1	0	+1	+1.682
methanol (M)	wt %	14.8	25	40	55	65.2
sulfuric acid (S)	wt %	1.6	5	10	15	18.4
reaction time (T)	min	16	30	50	70	84

$$Y = \beta_0 + \sum_{i=1}^{k} \beta_i x_i + \sum_{i=1}^{k} \beta_{ii} x_i^2 + \sum_{i=1}^{k} \sum_{j=i+1}^{k} \beta_{ij} x_i x_j + \varepsilon \quad (2)$$

2.2.2. Experimental Procedure of EPB. To initiate the esterification process, 100 g of PBO was placed in a 250 mL beaker and heated to 60 °C. Methanol was then blended at 300 rpm on a stirrer until the mixture appeared homogeneous. Sulfuric acid was gradually added, and the timer was started immediately. It is important to note that the addition of sulfuric acid triggers an exothermic reaction; therefore, it must be carefully controlled to remain below 64.7 °C, the boiling point of methanol. To prevent a forward reaction, the reaction should be rapidly cooled in cold water when it reaches the end. The resulting product consists of crude EPB (CEPB) and generated wastewater, with the less-dense CEPB floating on top and the wastewater settling at the bottom. The CEPB was washed with water to remove any remaining methanol and sulfuric acid residues. After purification, it is referred to as EPB and its ME purity is evaluated using nuclear magnetic resonance (NMR) spectroscopy with a model: AVANCE NEO 500 MHz instrument from Bruker, Germany.

2.3. Blending of D−B−EPB. To create the D−B−EPB blended fuel, three components were mixed with biodiesel using a magnetic stirrer at 400 rpm at a temperature of 30 °C (room temperature) for 10 min until a homogeneous phase was achieved. The resulting phases in D−B−EPB were observed for different ranges of diesel (0−90 wt %), biodiesel (0−90 wt %), and EPB (10−90 wt %), and the results were depicted in a ternary diagram. The final blends of D−B−EPB were stored in glass bottles, and the lids were immediately closed to observe the phase behavior of the fuels after complete blending for 30 days. However, all blend fuels were kept motionless for 3 months to assess their long-term stability at room temperature.

https://doi.org/10.1021/acsomega.3c05007
ACS Omega 2023, 8, 44586−44600

Table 3. Experimental Design and the ME Purity Results from the Esterification Process[a]

				ME (wt %)		
experiments	M (wt %)	S (wt %)	T (min)	actual	predicted	error
1	14.8	10.0	50	66.45	65.86	0.59
2	25.0	5.0	30	57.14	56.84	0.30
3	25.0	5.0	70	63.69	63.24	0.45
4	25.0	15.0	30	68.97	70.21	−1.24
5	25.0	15.0	70	71.43	71.63	−0.20
6	40.0	1.6	50	56.02	57.58	−1.56
7	40.0	10.0	16	65.33	65.05	0.28
8	40.0	10.0	50	71.17	71.19	−0.02
9	40.0	10.0	50	71.17	71.19	−0.02
10	40.0	10.0	50	71.22	71.19	0.03
11	40.0	10.0	50	71.26	71.19	0.07
12	40.0	10.0	84	70.92	71.70	−0.78
13	40.0	18.4	50	73.08	72.04	1.04
14	55.0	5.0	30	62.77	62.06	0.71
15	55.0	5.0	70	69.92	68.46	1.46
16	55.0	15.0	30	70.92	70.86	0.06
17	55.0	15.0	70	72.20	72.28	−0.08
18	65.2	10.0	50	69.69	70.79	−1.10

[a]Note: M is methanol, S is sulfuric acid, T is the reaction time, ME is the methyl ester purity.

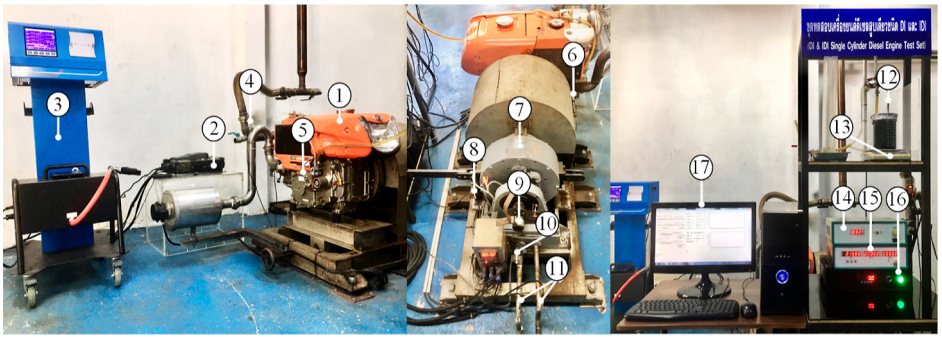

Figure 2. Diesel engine test rig: (1) DI engine; (2) exhaust gas analyzer; (3) smokemeter; (4) air temperature sensor; (5) engine oil temperature sensor; (6) EGT sensor; (7) dynamometer; (8) strain gauge load cell; (9) rotary encoder; (10) electric contact pressure gauge; (11) water temperature sensor; (12) fuel temperature sensor; (13) digital scale; (14) load controller; (15) control panel; (16) data logger; and (17) computer screen.

2.4. Fuel Property Testing. Table 1 presents the fuel characteristics of diesel, biodiesel, EPB, and fuel blends. These properties were measured using a hydrometer in accordance with ASTM D1298-12b, and viscosity was determined using a viscosity bath (model: Julabo Visco Bath ME-16G, Julabo Labortechnik GmbH; Seelbach, Germany) following ASTM D445-17a. The water content was measured using a volumetric Karl Fischer titrator (model: Mettler-Toledo V30S; Switzerland) in accordance with EN ISO 12937. The cloud point and pour point were determined using a cloud and pour point analyzer (model: Herzog CPP 97-2 device; Germany) as per ASTM D2500 and ASTM D97, respectively. The acid value, measured in milligrams of KOH/g, was determined through titration following ASTM D664-09. Copper strip corrosion was assessed by using a Herzog HZ9011 instrument according to ASTM D130-04. The higher heating value and LHV were determined using a CHNS/O analyzer (model: Flash 2000; Thermo Scientific; Italy). The purity of ME was analyzed using an NMR spectrometer (model: AVANCE NEO 500 MHz; Bruker, Germany) according to EN 14103. The ME of EPB after the esterification process was analyzed using a Fourier transform NMR analyzer on a ^{1}H NMR spectrometer operating at 500 MHz, with $CDCl_3$ as the solvent. The methanol content was determined using a gas chromatograph (model: 6850, Hewlett-Packard; USA) following EN 14110.

2.5. Diesel Engine Testing. The experimental setup involved a Kubota RT 100 DI diesel engine (model), as shown in Figure 2. The engine operated with a compression ratio of 18:1 and followed air-standard diesel cycles. The maximum power and engine speed were 7350 W and 2400 rpm, respectively. The maximum torque was 33.34 N m at an engine speed of 1600 rpm. The engine had a bore/stroke of 88 mm/90 mm, a displacement volume of 547 cm^3, a horizontal cylinder arrangement, an injection timing of 15−17° BTDC, and an injection pressure of 220 kg/cm^2. To simulate different engine loads, a dynamometer (model: DW 16, Jiangsu Lan Ling Test Equipment Co., Ltd.) was utilized. The eddy current dynamometer had a maximum power of 16 kW, a maximum torque of 70 N m, and a maximum speed of 13,000 rpm. It had a maximum voltage of 80 V and a maximum current of 3.5 A. The cooling water pressure ranged from 0.02 to 0.05 MPa, and the cooling water flow rate was 6.5 L/min. Further details of the diesel engine and eddy current dynamometers are provided in Table 4.

https://doi.org/10.1021/acsomega.3c05007
ACS Omega 2023, 8, 44586−44600

Table 4. Technical Specifications of the Test Engine and Dynamometer

engine characteristics	specification	dynamometer characteristics	specification
model	RT 100 DI	model	DW 16
type of engine	4-stroke, cooling with water	type of dynamometer	eddy current brake
type of combustion	direct injection	maximum power	16 kW
method of charging	naturally aspirated	maximum torque	70 N m
number of cylinders	1	maximum speed	13,000 rpm
cylinder arrangement	horizontal	turning inertia	0.02 kg m^2
compression ratio	18:1	maximum voltage	80 V
bore/stroke	88 mm/90 mm	maximum current	3.5 A
displacement volume	547 cm^3	cooling water pressure	0.02−0.05 MPa
maximum power	7.35 kW, 2400 rpm	flow of cooling water	6.5 L/min
maximum torque	33.34 N m, 1600 rpm		
maximum speed	2400 rpm		
injection timing	15−17° BTDC		
injection pressure	220 kg/cm^2		

For emissions analysis, the exhaust gas analyzer (model: Testo 350 XL; Titisee-Neustadt; Germany) was used to measure CO, CO_2, NO_x emissions, and O_2. The smoke opacity was measured by a smokemeter (model: CAPELEC; CAP3201EX-GO; Montpellier; France) in the range of 0−99.9%. The fuel consumption rate for the diesel engine was determined in kilograms per hour at various speeds of 1100, 1400, 1700, 2000, and 2300 rpm, with loads of 25, 50, and 75%, using a digital scale. To analyze engine emissions, the emission unit conversion from vol % or ppm to g/kW·h was calculated using the following equations[39]

$$O_2(g/kW{\cdot}h) = 41.024 \times O_2(vol\ \%) \quad (3)$$

$$CO(g/kW{\cdot}h) = 3.591 \times 10^{-3} \times CO(ppm) \quad (4)$$

$$CO_2(g/kW{\cdot}h) = 63.47 \times CO_2(vol\ \%) \quad (5)$$

$$NO_x(g/kW{\cdot}h) = 6.636 \times 10^{-3} \times NO_x(ppm) \quad (6)$$

2.6. Uncertainty Analysis. To determine the accuracy of the parameters and achieve reliable results, it is necessary to consider the uncertainty of the data obtained from the experiment. In the case of engine emissions, the uncertainty encompasses O_2, CO, CO_2, NO_x, EGT, and smoke opacity. Engine efficiency uncertainty, on the other hand, includes P_b, fuel consumption, BSFC, and BTE. P_b is calculated based on the uncertainty of engine speed and load, while fuel consumption is derived from the uncertainty of fuel weight, time, and fuel temperature. BSFC is determined by considering the uncertainty of P_b and fuel consumption, while BTE considers the uncertainty of LHV and BSFC. The measuring range, accuracy, and uncertainty data are presented in Table 5. Consequently, the overall experimental uncertainty can be estimated to be approximately ±1.04%. In summary, the overall experimental uncertainty is

$$\begin{aligned} &= [\text{uncertainty of}\{(O_2)^2 + (CO)^2 + (CO_2)^2 + (NO_x)^2 \\ &\quad + (EGT)^2 + (\text{Smoke opacity})^2 + (BTE)^2\}]^{1/2} \\ &= [\text{uncertainty of}\{(0.05)^2 + (0.01)^2 + (0.13)^2 + (0.02)^2 \\ &\quad + (0.01)^2 + (0.04)^2 + (1.03)^2\}]^{1/2} \\ &= \pm 1.04\% \end{aligned}$$

3. RESULTS AND DISCUSSION

3.1. Prediction Model and Statistical Analysis of the RSM. Prediction models were developed using RSM analysis

Table 5. Percentage Uncertainties of Various Instruments

measurement parameter	measuring range	instrument	accuracy	uncertainty (%)
		Measured Variables		
O_2 (vol %)	0 to 25 vol %	emission analyzer	±0.8%	±0.05
CO (ppm)	0 to 10,000 ppm	emission analyzer	±5%	±0.01
CO_2 (vol %)	0 to 25 vol %	emission analyzer	±0.8%	±0.13
NO_x (ppm)	0 to 3000 ppm	emission analyzer	±5%	±0.02
EGT (°C)	0 to 1000 °C	temperature sensor	±2.6%	±0.01
smoke opacity (%)	0 to 99.9%	smoke analyzer	±0.1	±0.04
engine speed (rpm)	0 to 6000 rpm	rotary encoder	±10 rpm	±0.17
fuel weight (g)	0 to 300 g	digital scale	±0.02 g	±0.01
time (s)	-	digital stopwatch timer	±0.1 s	±0.08
fuel temperature (°C)	250 to 1300 °C	temperature sensor	±2.6 °C	±0.20
load (Nm)	0 to 70 N m	strain gauge load cell CHNS/O analyzer	±0.1%	±0.01
LHV (kJ/kg)				±0.56
		Calculated Parameters		
P_b[a] (W)				±0.18
fuel consumption[b] (kg/h)				±0.29
BSFC[c] (kg/kW·h)				±0.47
BTE[d] (%)				±1.03

[a]The uncertainty of P_b is [(uncertainty of engine speed) + (uncertainty of load)], is equal to [(0.17) + (0.01)] = ± 0.18%. [b]The uncertainty of fuel consumption is [(uncertainty of fuel weight) + (uncertainty of time) + (uncertainty of fuel temperature)], is equal to [(0.01) + (0.08) + (0.2)] = ± 0.29%. [c]The uncertainty of BSFC is [(uncertainty of P_b) + (uncertainty of fuel consumption)], is equal to [(0.18) + (0.29)] = ± 0.47%. [d]The uncertainty of BTE is [(uncertainty of LHV) + (uncertainty of BSFC)], is equal to [(0.56) + (0.47)] = ± 1.03%.

https://doi.org/10.1021/acsomega.3c05007
ACS Omega 2023, 8, 44586−44600

to identify the optimal conditions for ME production from EPB by evaluating the correlation between independent and dependent variables. The experiments yielded ME purities ranging from 56.02 to 73.08 wt %, as shown in Table 3. A second-degree polynomial model was used to predict ME production from EPB. Multiple regression analysis was used to fit models from 18 experiments with a Microsoft Excel add-in tool, as detailed in Table 6. Table 6 shows the coefficient values, *p*-values, and analysis of variance (ANOVA) for ME generation of eq 7. At a 95% confidence level, *p*-values of each coefficient of less than 0.05 were considered statistically significant in the predicted model. The purity of ME was found to depend on the methanol content, sulfuric acid content, and reaction time, which were examined using complete multiple regression techniques at a 95% confidence level. Equation 7 presents the predicted model for the correlation between the ME purity and the three parameters. The coefficient of determination (R^2) and adjusted coefficient of determination ($R^2_{adjusted}$) values for ME purity were 0.976 and 0.956, respectively. The regression coefficients, *p*-values, and ANOVA for ME production are shown in Table 6. In the predictive model, coefficients with *p*-values less than 0.05 were considered statistically significant at a 95% confidence level. The terms $\beta_2 S$ and $\beta_6 S^2$ in eq 7 had the lowest *p*-values in the correlation prediction model, indicating that sulfuric acid content significantly impacted ME purity in EPB. The influences of reaction time and methanol content were denoted by the terms $\beta_3 T$ and $\beta_1 M$, respectively, ranking third and fourth. The *F*-test results showed that the F_0 value of 46.7 exceeded the F_{crit} value of 3.23 ($F_{0.05,8,9}$) at a 95% confidence level, as shown in Table 6. Thus, the correlation prediction equation for the ME purity was statistically significant. Moreover, the number of experiments was adequate for examining how the independent variables affected the increase in the ME purity. The correlation between the anticipated and the actual experimental ME purity is demonstrated in Figure 3. The results confirmed that the appropriate model can be used to observe the ME purity rising. Additionally, R^2 and $R^2_{adjusted}$ were used to assess the model's validity. Both coefficients were very close to 1, confirming that the model was highly significant and that the degree of correlation between the dependent and independent variables was acceptable. In addition, as shown in Table 3, the comparisons of the observed and expected values showed a satisfactory level of agreement. These statistical tests indicated that the preferred model provided reliable predictions of ME purity across all of the tested parameters in the experiments.

Table 6. Values of Coefficients and ANOVA of the Prediction Model[a]

coefficient	value	*p*-value
β_0	19.1932	0.0017660
β_1	0.6094	0.0006592
β_2	3.8951	0.0000024
β_3	0.4653	0.0003700
β_4	−0.0045	0.0084233
β_5	−0.0152	0.0144530
β_6	−0.0902	0.0000373
β_7	−0.0125	0.0093460
β_8	−0.0024	0.0094154
R^2	0.976	
$R^2_{adjusted}$	0.956	

source	SS	MS	F_0	F_{signif}	DOF
regression	427.4413	53.4302	46.7	3.23 ($F_{0.05,8,9}$)	8
residual	10.2969	1.1441			9
LOF error	10.2912	1.7152	902.7	8.94 ($F_{0.05,6,3}$)	6
pure error	0.0057	0.0019			3
total	437.7382				17

[a]Note: SS, sum of squares; MS, mean square; F_0, test statistic; F_{signif}, *F*-table of critical values for a significance level of 0.05; LOF, lack-of-fit; and DOF, degrees of freedom.

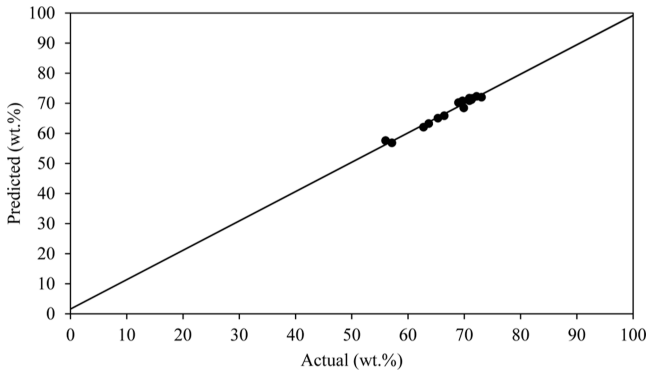

Figure 3. Comparison of ME purity increment results between predicted and actual experiments.

$$ME = \beta_0 + \beta_1 M + \beta_2 S + \beta_3 T + \beta_4 M^2 + \beta_5 MS + \beta_6 S^2 + \beta_7 ST + \beta_8 T^2 \quad (7)$$

where ME is the methyl ester purity (wt %), *M* is methanol (wt %), *S* is sulfuric acid (wt %), *T* is the reaction time (min), and β is the coefficient value.

3.2. Response Surface Plots and Optimal Condition. The relationships between the dependent variable (ME) and independent variables (methanol, sulfuric acid, and reaction time) in the production of ME from EPB are shown as contour plots in Figure 4. The solver function in Microsoft Excel was utilized to determine the optimal conditions for ME production from EPB. These optimal conditions were then employed to produce ME from EPB, which was subsequently analyzed using the NMR method. The highest purity of ME, amounting to 73.50 wt %, was achieved under the optimal conditions predicted by the model, which entailed 44.8 wt % methanol, 13.6 wt % sulfuric acid, and a 61 min reaction time. To validate the accuracy of the predicted model, the optimal conditions were implemented in an actual experiment to verify the purity of ME. The experimental results yielded a ME purity of 73.26 wt %, which closely aligned with the values obtained from the prediction model. This confirms that the prediction model exhibits a high level of confidence in the production of ME through the esterification process from EPB.

3.3. Phase Stability of D−B−EPB. Figure 5 illustrates the phase separation behavior of D−B−EPB at 30 °C after 30 days, with symbols representing different characteristics: (◯) liquid one-phase, (□) liquid two-phase, (△) acceptable density of fuel blend, and (▲) acceptable density and viscosity of fuel blend. The phase separation behavior can be categorized into two types: liquid one-phase and liquid two-phase. A one-phase liquid refers to a homogeneous liquid without any separating layer or suspended particles. On the other hand, the liquid two-phase consists of two distinct layers: a dark green top layer and a dark brown bottom layer.

https://doi.org/10.1021/acsomega.3c05007
ACS Omega 2023, 8, 44586−44600

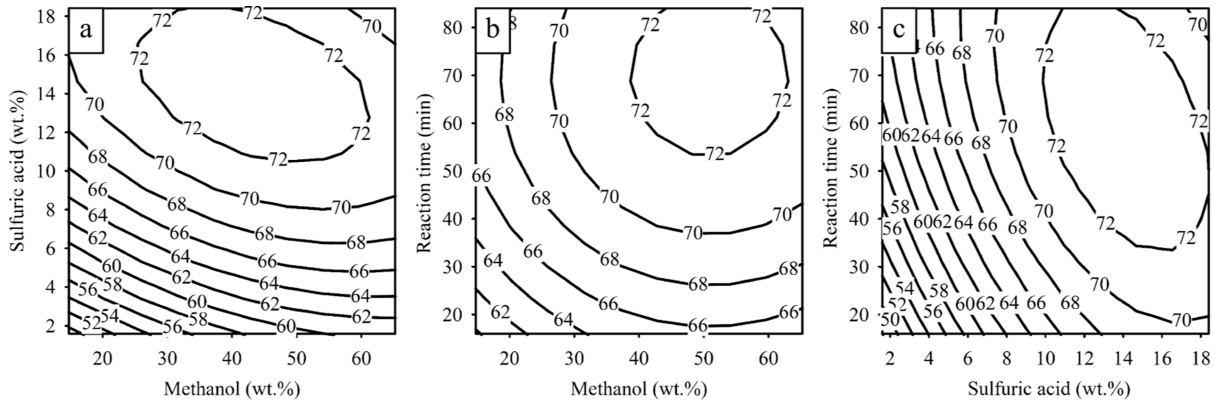

Figure 4. Contour plots of the effects of the three parameters on the ME purity in EPB: (a) methanol and sulfuric acid, (b) methanol and reaction time, and (c) sulfuric acid and reaction time.

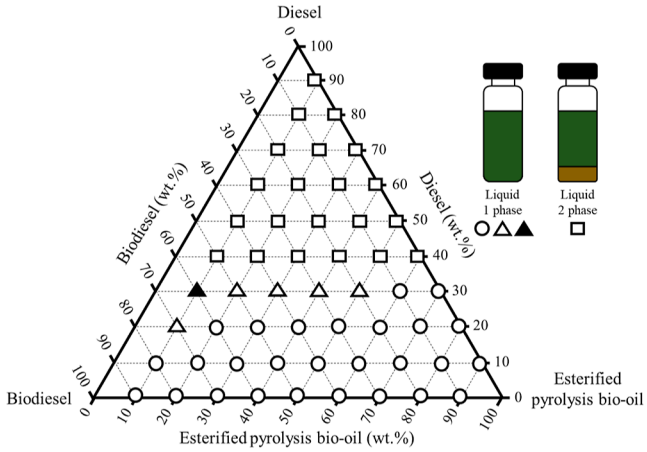

Figure 5. Phase behavior of D−B−EPB, (◯) liquid one-phase, (□) liquid two-phase, (△) acceptable density of fuel blend, and (▲) acceptable density and viscosity of fuel blend.

Observation of the phase separation behavior of D−B−EPB reveals that the blend fuels exhibit no phase separation (liquid one phase) in 33 out of 54 conditions, while phase separation (liquid two phase) occurs in the remaining 21 conditions. Further analysis of the liquid one-phase conditions or homogeneous regions, considering the homogeneous regions of proportion of diesel (0−30 wt %), biodiesel (0−90 wt %), and EPB (10−90 wt %), indicates that a proportion of diesel exceeding 30 wt % leads to liquid two-phase or heterogeneous region formation and faster phase separation. This can be attributed to the better compatibility of EPB with biodiesel compared with diesel. Hence, the phase separation behavior is more prolonged when the proportion of diesel is below 30 wt %. The liquid two-phase conditions consider the heterogeneous regions of proportion of diesel (40−90 wt %), biodiesel (0−50 wt %), and EPB (10−60 wt %). The properties of density and viscosity for the liquid one-phase were also examined. It was observed that the density of the liquid one-phase met the diesel standard within the range of 810−870 kg/m^3 under six conditions. Similarly, the viscosity of the liquid one-phase met the diesel standard within the range of 1.8−4.1 cSt at 40 °C, with only one condition (D30B60EPB10) meeting the criteria. This blended fuel consists of 30% diesel, 60% biodiesel, and 10% EPB. Consequently, this blend will undergo testing in an unmodified diesel engine at various engine speeds and loads to analyze its performance and exhaust gas emissions. Table 1 presents the fuel characteristics of diesel, biodiesel, EPB, and D30B60EPB10.

3.4. Engine Performance. *3.4.1. Brake Power.* P_b is the actual power obtained at the crankshaft and is always lower than the indicated power.[40] P_b is a product of torque and angular speed, and an increase in P_b can be attributed to increased torque and angular speed.[41] Figure 6a illustrates the P_b for diesel, biodiesel, and D30B60EPB10 at different engine speeds. As the engine speed increased to 2300 rpm, the P_b values of all fuels also increased. However, the P_b values of biodiesel and D30B60EPB10 were slightly lower than that of diesel at all speeds. When P_b was compared at a maximum engine speed of 2300 rpm and diesel exhibited the highest P_b level, followed by D30B60EPB10 and biodiesel. This can be attributed to the higher viscosity and density of biodiesel and D30B60EPB10 compared with diesel, which leads to decreased fuel combustion efficiency due to poor atomization,[42,43] as shown in Table 1. Furthermore, the LHV of biodiesel and D30B60EPB10 is also lower than that of diesel, resulting in lower P_b.[42,44] Mofijur et al.[44] reported that the lower P_b of biodiesel blend compared with that of diesel is due to its lower calorific value and higher viscosity, which result in uneven combustion characteristics and decreased P_b.

3.4.2. Brake-Specific Fuel Consumption. BSFC is defined as the ratio of fuel consumed per hour to produce 1 kW of P_b. Various physiochemical characteristic factors impact engine fuel consumption, including density, viscosity, heating value, and cetane number.[45] Figure 6b illustrates the variation in BSFC for diesel, biodiesel, and D30B60EPB10 at different engine speeds and loads. Biodiesel exhibits the lowest LHV, resulting in the highest BSFC at all engine speeds and loads. When comparing all fuel types, it was observed that both biodiesel and D30B60EPB10 have higher BSFC than diesel due to their lower LHV, necessitating more fuel to achieve the same level of P_b. Midhun Prasad and Murugavelh[46] reported that the BSFC of tomato pyrolysis oil blend (TPO) was higher than that of diesel due to its higher mass and lower calorific value. The lower calorific value can explain the higher BSFC of the TPO blends. When comparing biodiesel and D30B60EPB10, the BSFC of D30B60EPB10 was lower than biodiesel due to its higher LHV. Additionally, the higher density and viscosity of biodiesel and D30B60EPB10 lead to larger droplets and hinder vaporization in the combustion chamber during the injection stage, resulting in increased BSFC. Subramanian et al.[47] reported that the BSFC of the PBO blend was higher than that of diesel due to its higher

https://doi.org/10.1021/acsomega.3c05007
ACS Omega 2023, 8, 44586−44600

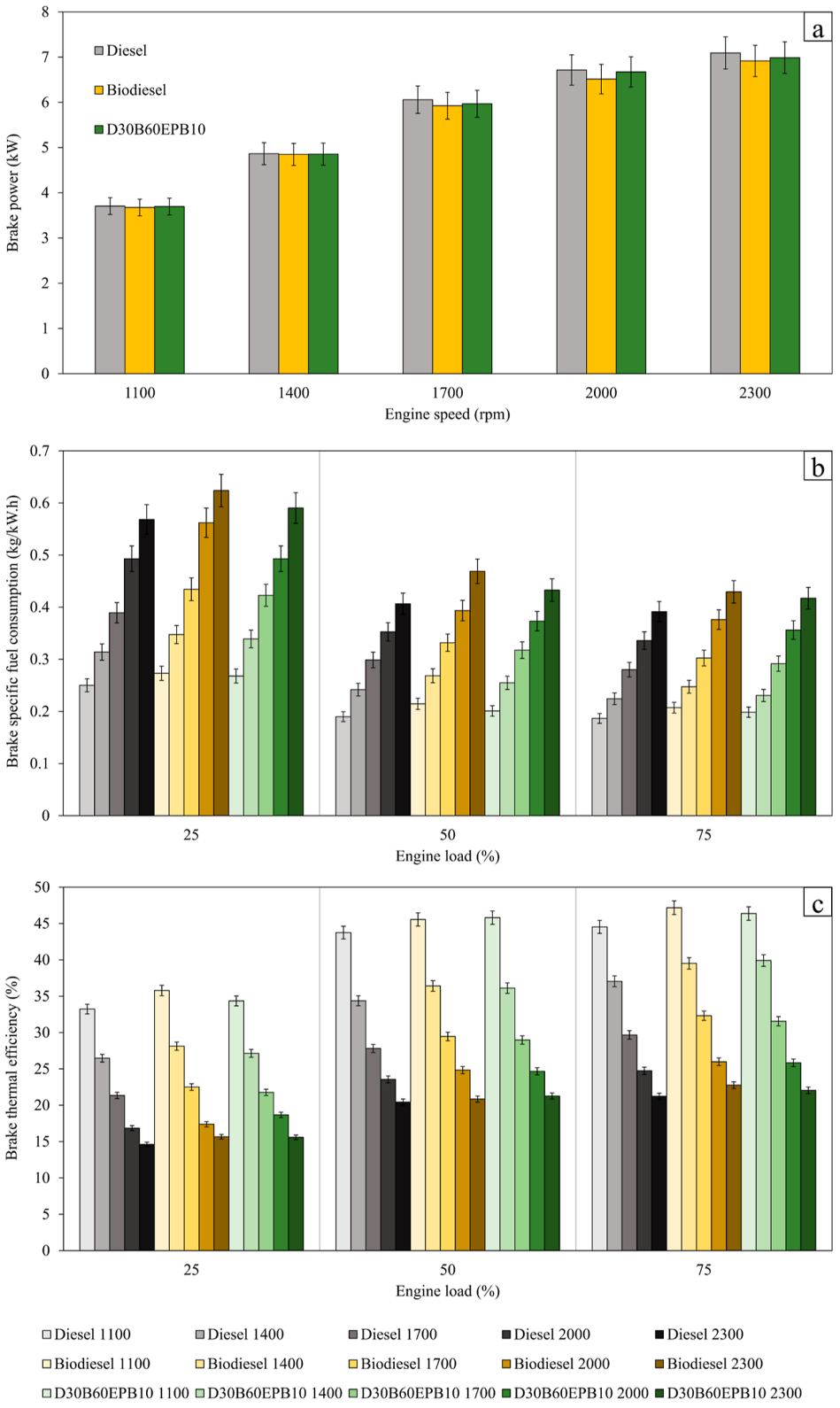

Figure 6. Effect of all fuels on the performance of diesel engines operating at various engine speeds and loads: (a) P_b, (b) BSFC, and (c) BTE.

density. Higher density values can account for the higher BSFC values of PBO blends. Comparing biodiesel and D30B60EPB10, the BSFC of the blend was lower than that of biodiesel due to its lower density and viscosity. At 25, 50, and 75% engine load, the BSFC of D30B60EPB10 closely resembled that of biodiesel, as D30B60EPB10 had a calorific value similar to biodiesel. At 25% engine load and 2300 rpm speed, the BSFCs of biodiesel and D30B60EPB10 were 9.76 and 3.87% higher than that of diesel, respectively. Compared with biodiesel, the BSFC of D30B60EPB10 was 5.37% lower. At 50% engine load and 2300 rpm, the BSFCs of biodiesel and D30B60EPB10 were 15.32 and 6.44% higher than that of

https://doi.org/10.1021/acsomega.3c05007
ACS Omega 2023, 8, 44586−44600

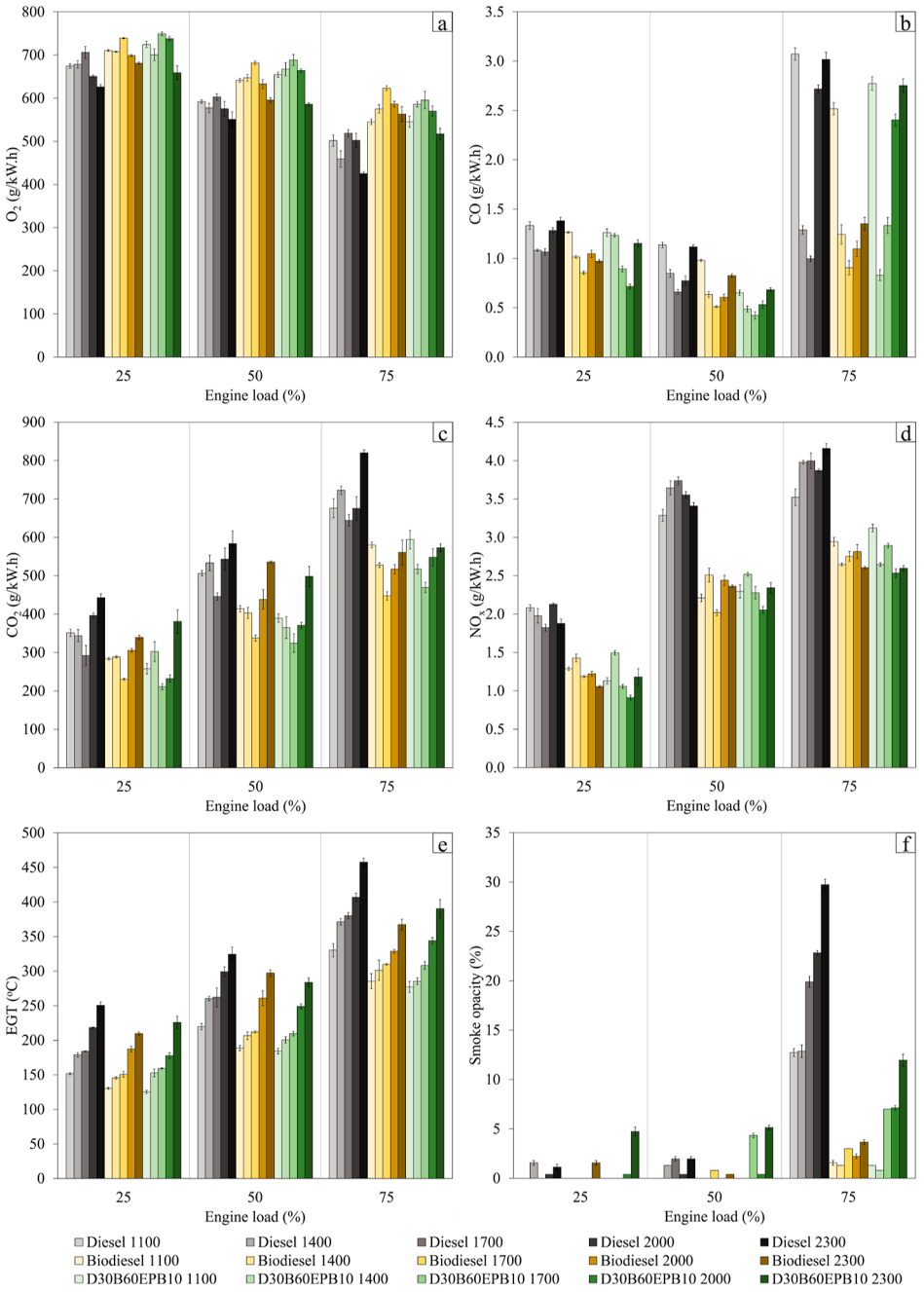

Figure 7. Effect of emissions on combustion in diesel engine: (a) O_2, (b) CO, (c) CO_2, (d) NO_x, (e) EGT, and (f) smoke opacity.

diesel, respectively. Compared with biodiesel, the BSFC of D30B60EPB10 was 7.70% lower. At 75% engine load, the BSFC of biodiesel was higher than that of diesel. The BSFC values were found to be 11.03, 10.26, 7.97, 11.94, and 9.71% for 1100, 1400, 1700, 2000, and 2300 rpm, respectively. Similarly, the BSFC of D30B60EPB10 was higher, with values of 6.36, 2.80, 4.11, 6.02, and 6.60% for 1100, 1400, 1700, 2000, and 2300 rpm, respectively. Compared with biodiesel, the BSFC of D30B60EPB10 was lower, with values of 4.21, 6.77, 3.58, 5.29, and 2.84% for 1100, 1400, 1700, 2000, and 2300 rpm, respectively.

3.4.3. Brake Thermal Efficiency. BTE is a significant parameter that describes the efficient conversion of thermal energy released from fuel combustion into useful mechanical energy.[48] Figure 6c illustrates the BTEs of three fuels at various engine speeds and loads. The BTEs of biodiesel and D30B60EPB10 were higher than those of diesel at all engine speeds and loads. The presence of oxygen in biodiesel and D30B60EPB10 improves combustion efficiency and oxidation, thereby increasing the BTE. Yadav et al.[49] reported that the BTE of the biodiesel blend was higher than that of diesel, possibly due to the oxygen content in the biodiesel blend, resulting in better combustion compared with diesel. Similarly, Baranitharan et al.[50] reported that the BTE of the PBO blend was higher than that of diesel, attributed to the high oxygen content in the PBO blend, which enhances the combustion process and lowers fuel consumption, ultimately achieving higher BTE than diesel. At a 25% engine load, the BTE for D30B60EPB10 was comparable to that of diesel across all speeds. At speeds ranging from 1100 to 2300 rpm, the BTE of

https://doi.org/10.1021/acsomega.3c05007
ACS Omega 2023, 8, 44586−44600

D30B60EPB10 was comparable to that of diesel, and as the engine speed increased, the BTE of D30B60EPB10 surpassed that of diesel. At a 25% engine load and 2300 rpm, the BTEs for biodiesel and D30B60EPB10 were 7.14 and 6.61% higher than that of diesel, respectively. Compared to biodiesel, the BTE of D30B60EPB10 was 0.49% lower. At a 50% engine load and 2300 rpm, the BTEs of biodiesel and D30B60EPB10 were 1.98 and 4.04% higher than that of diesel, respectively. Compared with biodiesel, the BTE of D30B60EPB10 was 2.02% higher. At a 75% engine load, the BTE of biodiesel was greater than that of diesel. The BTE values were 5.92, 6.65, 8.92, 5.05, and 7.19% for speeds of 1100, 1400, 1700, 2000, and 2300 rpm, respectively. D30B60EPB10 exhibited a higher BTE, with values of 4.12, 7.72, 6.36, 4.44, and 3.88% for speeds of 1100, 1400, 1700, 2000, and 2300 rpm, respectively. However, D30B60EPB10 had a lower BTE compared with biodiesel, with values of 1.70, 2.34, 0.58, and 3.08% for speeds of 1100, 1700, 2000, and 2300 rpm, respectively.

3.5. Engine Emission. *3.5.1. Oxygen Gas.* The O_2 content in exhaust gases serves as an indicator of combustion quality.[51] Figure 7a shows the relationship between engine load and O_2. O_2 represents the amount of oxygen remaining after combustion. As engine load increases, O_2 decreases because more fuel and air are required for complete combustion.[52] Consequently, the engine operates with a rich fuel-to-air ratio under high load conditions, and oxygen is consumed in the generation of H_2O, CO_2, and NO_x.[53] When comparing the O_2 content of each fuel, it was found that biodiesel and D30B60EPB10 emitted more O_2 than diesel due to their higher oxygen levels.[54] At 25% engine load and 2300 rpm maximum speed, biodiesel and D30B60EPB10 emit more O_2 than diesel at 8.74 and 5.19%, respectively. At 50% engine load and 2300 rpm engine speed, biodiesel and D30B60EPB10 emit more O_2 than diesel at 8.11 and 6.41%, respectively. At 75% maximum engine load and 2300 rpm speed, biodiesel and D30B60EPB10 emit more of the O_2 than diesel at 32.46 and 21.65%, respectively. Gumus et al.[55] confirmed a similar trend, indicating that the addition of a higher amount of biodiesel to diesel increases the amount of O_2. Typically, diesel engines operate under fuel-lean combustion conditions. Excess air naturally enters the combustion chamber during engine operation to mix with the atomized droplets of biodiesel during fuel injection. The chemically bound oxygen in biodiesel contributes to an increased amount of excess oxygen in the reactant mixture. As a result, biodiesel combustion generates more residual O_2 than diesel combustion, leading to higher levels of O_2 in exhaust gases.

3.5.2. Carbon Monoxide Emission. The intermediate product of combustion is CO, which is formed through the incomplete oxidation of fuel during the combustion process. On the other hand, CO_2 is produced when full combustion takes place.[56] CO emissions are a significant source of pollution and represent an inefficient use of energy from the combustion process. The fuel-air equivalency ratio is the most critical factor that influences CO emissions.[57] Figure 7b illustrates the relationship between engine load and CO emissions. As the engine load increases, CO emissions decrease at 25 and 50% engine load, respectively. However, at 75% engine load, CO emissions rise due to increased fuel consumption, resulting in a rich air−fuel mixture. In a comparison of the three fuels, biodiesel and D30B60EPB10 emit less CO than diesel because their higher oxygen content enables more efficient combustion.[58] At 25% load and 2300 rpm speed, biodiesel and D30B60EPB10 released 29.58 and 16.54% less CO than diesel, respectively. At 50% load and 2300 rpm speed, biodiesel and D30B60EPB10 emitted 26.08 and 38.83% less CO than diesel, respectively. For a 75% engine load and 2300 rpm speed, biodiesel and D30B60EPB10 emitted 55.19 and 8.73% less CO than diesel, respectively. In terms of emissions, Paramasivam et al.[33] also described that the CO emission of bio-oil blends was lower than that of diesel under all engine loads. The type of fuel, engine load, and air/fuel ratio directly affect the CO emissions of exhaust gases in the engine. The increased ignition delay period and slow burning at low loads result in less air−fuel oxidation. Operating a diesel engine at a high air−fuel ratio leads to low CO emissions. These results suggest that bio-oil blends are a viable biofuel option for diesel engines to reduce the level of pollution in the environment.

3.5.3. Carbon Dioxide Emissions. CO_2 is one of the greenhouse gases emitted by an engine during the complete combustion of fuel. The increase in CO_2 emissions indicates the degree of complete combustion in the power stroke.[59] Figure 7c shows the relationship between engine load and CO_2 emissions. As the engine load increases, CO_2 emissions also increase due to higher fuel consumption at higher loads. In a comparison of the three fuels, biodiesel and D30B60EPB10 emitted less CO_2 than diesel. This can be attributed to the lower specific hydrogen-to-carbon ratio (H/C) and higher oxygen content in biodiesel and D30B60EPB10, which improve engine combustion.[60] At 25% load and 2300 rpm speed, biodiesel and D30B60EPB10 released 23.33 and 14.00% less CO_2 than diesel, respectively. At 50% load and 2300 rpm speed, biodiesel and D30B60EPB10 emitted 8.21 and 14.62% less CO_2 than diesel, respectively. For a 75% load and 2300 rpm speed, the biodiesel and D30B60EPB10 emitted 31.62 and 30.13% less CO_2 than diesel, respectively. In terms of emissions, Mohapatra et al.[61] studied copyrolytic oil obtained from sugar cane bagasse and polystyrene in a CI engine. They observed an increase in CO_2 emissions as the engine load increased due to proper injection of the air/fuel ratio in the combustion chamber. However, the CO_2 emissions decreased as the proportion of copyrolytic oil blends increased. The CO_2 emissions of copyrolytic oil blends were reduced compared with diesel due to poor fuel injection and higher viscosity, resulting in incomplete oxidation of CO. For CO_2 emissions, they concluded that copyrolytic oil at 5, 10, and 15% in diesel released 10.52, 5.20, and 7.89% less CO_2 than diesel, respectively.

3.5.4. Nitrogen Oxide Emissions. The majority of NO_x emitted by diesel engines consists of nitric oxide and nitrogen dioxide. The levels of NO_x in diesel engine exhaust gases are influenced by various parameters including fuel composition, air−fuel ratio, and combustion temperature. However, numerous studies have indicated that combustion temperature is the most significant factor.[62] Figure 7d illustrates the relationship between engine load and nitrogen oxide emissions. As the engine load increases, there is a characteristic increase in NO_x emissions due to rising temperatures in the combustion chamber. A comparison of each fuel revealed that biodiesel and D30B60EPB10 had NO_x emissions lower than diesel. The formation of NO_x depends on the amounts of N_2 and O_2. However, the higher density and viscosity of biodiesel and D30B60EPB10 contribute to delayed combustion. The substantial reduction in NO_x emissions suggests that biodiesel and D30B60EPB10 burn at lower temperatures.[63,64] At 25%

https://doi.org/10.1021/acsomega.3c05007
ACS Omega 2023, 8, 44586−44600

engine load and 2300 rpm engine speed, biodiesel and D30B60EPB10 emitted 43.76 and 37.16% less NO_x than diesel, respectively. At 50% engine load and 2300 rpm engine speed, biodiesel and D30B60EPB10 emitted 30.66 and 31.28% less NO_x than diesel, respectively. At 75% engine load and 2300 rpm engine speed, biodiesel and D30B60EPB10 emitted 37.37 and 37.55% less NO_x than diesel, respectively. Similar findings were reported by Geng et al.,[65] who stated that NO_x emissions from engines depend on the residence time at elevated temperatures in the cylinder, the air-to-fuel ratio, and the combustion temperature. NO_x emissions were significantly reduced in diesel blends containing 70, 90, and 100% biodiesel due to the higher cetane number of biodiesel, resulting in shorter premixed combustion and ignition delays. Lower cylinder temperatures also contribute to the reduction of the NO_x emissions during the combustion process.

3.5.5. Exhaust Gas Temperature. EGT serves as an indicator of combustion in the engine. Figure 7e illustrates the relationship between engine load and EGT. When comparing the EGT of the three fuels, it was observed that diesel exhibited higher EGT values compared with biodiesel and D30B60EPB10. The presence of oxygen in biodiesel reduces the duration of the premixed combustion and increases the cetane number. This shift in ignition delay leads to a decrease in the EGT as the proportion of biodiesel in the blend increases. Longer ignition delays may result in slower combustion and higher EGT.[63] In another study, Sukumar et al.[34] found that the use of bio-oil blends influenced the duration of the delay, with shorter delay periods leading to delayed combustion and decreased EGT. At a 25% engine load and 2300 rpm engine speed, biodiesel and D30B60EPB10 exhibited lower EGT values compared with diesel, with reductions of 16.33 and 9.90%, respectively. Similarly, at a 50% engine load and 2300 rpm engine speed, biodiesel and D30B60EPB10 emitted lower EGT values than diesel, with reductions of 8.32 and 12.54%, respectively. For a 75% load and 2300 rpm speed, biodiesel and D30B60EPB10 resulted in lower EGT values compared with diesel with reductions of 19.76 and 14.72%, respectively. Similar findings were reported by Asokan et al.,[66] who observed that an increase in engine load leads to an increase in EGT. Due to poor combustion characteristics and viscosity, the EGT of diesel blends containing 20, 30, 40, and 100% biodiesel is lower than that of pure diesel.

3.5.6. Smoke Opacity. Smoke opacity refers to the extent to which smoke obstructs the passage of light. A higher level of smoke in the exhaust gas corresponds to increased smoke opacity.[67] Smoke is generated when solid carbon soot particles form in the rich fuel zone during cylinder combustion.[68] The relationship between the engine load and smoke opacity is shown in Figure 7f. While 25 and 50% engine loads exhibited relatively low smoke opacity, incomplete combustion occurred at 75% load due to greater fuel injection resulting in higher emissions, compounded by increased engine load. Upon evaluating each fuel, it was observed that biodiesel and D30B60EPB10 emitted less smoke compared with diesel. The higher oxygen and lower carbon content in biodiesel facilitated improved combustion, particularly when a significant amount of oxygen was present in the fuel. Another study indicated that a higher concentration of oxygen and OH in the blend enhanced combustion and minimized smoke emissions.[29] At 75% load and 2300 rpm speed, biodiesel and D30B60EPB10 emitted 87.67 and 59.75% less smoke than diesel, respectively. Similar findings were reported by Mulimani and Navindgi[69] investigated the impact of oxygen in bio-oil, cylinder air pressure, and fuel type on smoke. The greater oxygen content of the bio-oil blend allowed for increased utilization of oxygen during the fuel combustion process, resulting in reduced smoke emissions.

4. CONCLUSIONS

The PBO was upgraded through the esterification process, resulting in EPB as confirmed by RSM. Subsequently, the phase separation behavior of D−B−EPB was analyzed using a ternary phase diagram, and the fuels were assessed against diesel standards. The blended fuel was then tested for performance and emissions on unmodified diesel engines at various speeds and loads. The results showed that esterification-based upgrading of PBO improved the density and viscosity of the upgraded bio-oil. The blended fuel, which met diesel standards in terms of density and viscosity, exhibited superior characteristics compared with those of conventional biodiesel. Considering both engine performance and emissions, D30B60EPB10 was identified as a potential fuel. It can be considered a fuel with a performance closest to diesel while being more environmentally friendly.

AUTHOR INFORMATION

Corresponding Author

Krit Somnuk − *Department of Mechanical and Mechatronics Engineering, Faculty of Engineering, Prince of Songkla University, Hat Yai, Songkhla 90110, Thailand; Energy Technology Research Center, Faculty of Engineering, Prince of Songkla University, Hat Yai, Songkhla 90110, Thailand;* orcid.org/0000-0002-1771-5120; Email: krit.s@psu.ac.th

Authors

Sutthichai Khamhuatoey − *Department of Mechanical and Mechatronics Engineering, Faculty of Engineering, Prince of Songkla University, Hat Yai, Songkhla 90110, Thailand*

Sommas Kaewluan − *Mechanical Engineering Department, Faculty of Engineering, Srinakarinwirot University, Nakhonnayok 26120, Thailand*

Jarernporn Thawornprasert − *Department of Mechanical and Mechatronics Engineering, Faculty of Engineering, Prince of Songkla University, Hat Yai, Songkhla 90110, Thailand*

Ye Min Oo − *Department of Mechanical and Mechatronics Engineering, Faculty of Engineering, Prince of Songkla University, Hat Yai, Songkhla 90110, Thailand*

Kritsakon Pongraktham − *Department of Mechanical and Mechatronics Engineering, Faculty of Engineering, Prince of Songkla University, Hat Yai, Songkhla 90110, Thailand;* orcid.org/0000-0002-6919-0637

Complete contact information is available at: https://pubs.acs.org/10.1021/acsomega.3c05007

Notes

The authors declare no competing financial interest.

ACKNOWLEDGMENTS

This research was funded by the National Science, Research and Innovation Fund (NSRF) and Prince of Songkla University (grant no. ENG6505015M).

ABBREVIATIONS

BSFC	brake-specific fuel consumption
BTE	brake thermal efficiency
CEPB	crude esterified pyrolysis bio-oil
CO	carbon monoxide
CO_2	carbon dioxide
D30B60EPB10	30 wt % diesel +60 wt % biodiesel +10 wt % esterified pyrolysis bio-oil blended fuel
EGT	exhaust gas temperature
EPB	esterified pyrolysis bio-oil
FFA	free fatty acid
H_2SO_4	sulfuric acid
KOH	potassium hydroxide
LHV	lower heating value
CPO	crude palm oil
ME	methyl ester
NMR	nuclear magnetic resonance
NO_x	nitrogen oxides
O_2	oxygen gas
PBO	pyrolysis bio-oil
P_b	brake power
RSM	response surface methodology
vol %	percentage by volume
wt %	percentage by weight
SFC	specific fuel consumption

REFERENCES

(1) Cherubini, F. The biorefinery concept: Using biomass instead of oil for producing energy and chemicals. *Energy Convers. Manage.* **2010**, *51*, 1412−1421.

(2) Ministry of Energy. Biomass database potential in Thailand Home Page. http://weben.dede.go.th/webmax/content/biomass-database-potential-thailand (accessed June 2, 2023).

(3) U.S. Energy Information Administration. Biomass explained Home Page. https://www.eia.gov/energyexplained/biomass/ (accessed June 2, 2023).

(4) Demirbas, A. Biofuels securing the planet's future energy needs. *Energy Convers. Manage.* **2009**, *50*, 2239−2249.

(5) Kumar, G.; Dharmaraja, J.; Arvindnarayan, S.; Shoban, S.; Bakonyi, P.; Saratale, G. D.; Nemestóthy, N.; Bélafi−Bakó, K.; Yoon, J. J.; Kim, S. H. A comprehensive review on thermochemical, biological, biochemical and hybrid conversion methods of bio-derived lignocellulosic molecules into renewable fuels. *Fuel* **2019**, *251*, 352−367.

(6) Demirbas, A. Hydrogen-rich gas from fruit shells via supercritical water extraction. *Int. J. Hydrogen Energy* **2004**, *29*, 1237−1243.

(7) Landrat, M.; Abawalo, M. T.; Pikoń, K.; Turczyn, R. Bio-oil derived from teff husk via slow pyrolysis process in fixed bed reactor and its characterization. *Energies* **2022**, *15*, 9605.

(8) Figueirêdo, M. B.; Hita, I.; Deuss, P. J.; Venderbosch, R. H.; Heeres, H. J. Pyrolytic lignin: a promising biorefinery feedstock for the production of fuels and valuable chemicals. *Green Chem.* **2022**, *24*, 4680−4702.

(9) Makarfi Isa, Y.; Ganda, E. T. Bio-oil as a potential source of petroleum range fuels. *Renewable Sustainable Energy Rev.* **2018**, *81*, 69−75.

(10) Pandey, S. P.; Upadhyay, R.; Prakash, R.; Kumar, S. Performance and emission analysis of blends of bio-oil obtained by catalytic pyrolysis of Argemone mexicana seeds with diesel in a CI engine. *Environ. Sci. Pollut. Res.* **2022**, 1−14.

(11) Duku, M. H.; Gu, S.; Hagan, E. B. A comprehensive review of biomass resources and biofuels potential in Ghana. *Renewable Sustainable Energy Rev.* **2011**, *15*, 404−415.

(12) Shimizu, H.; Desrochers, P. The health, environmental and economic benefits of palm oil. *IEM's Economic Note* **2012**, 1−4.

(13) Fold, N.; Whitfield, L. *Developing a palm oil sector: the experiences of Malaysia and Ghana compared*; DIIS Working Paper, 2012.

(14) Biofuels international. Indonesia launches higher blend of palm oil-based biodiesel Home Page. https://biofuels-news.com/news/indonesia-launches-higher-blend-of-palm-oil-based-biodiesel/ (accessed Aug 4, 2023).

(15) Reuters. Indonesia, Malaysia commit to biodiesel mandates despite higher prices Home Page. https://www.reuters.com/business/sustainable-business/indonesia-malaysia-commit-biodiesel-mandates-despite-higher-prices-2022-03-24/ (accessed Aug 4, 2023).

(16) Enerdata. Malaysia targets full implementation of B20 biodiesel mandate by end-2022 Home Page. https://www.enerdata.net/publications/daily-energy-news/malaysia-targets-full-implementation-b20-biodiesel-mandate-end-2022.html (accessed Aug 4, 2023).

(17) Bank of Ayudhya Public Company Limited. Industry Outlook 2021−2023: Biodiesel Home Page. https://www.krungsri.com/en/research/industry/industry-outlook/energy-utilities/biodiesel/io/io-biodiesel-21 (accessed Aug 4, 2023).

(18) Bank of Ayudhya Public Company Limited. Industry Outlook 2022−2024: Palm Oil Industry Home Page. https://www.krungsri.com/en/research/industry/industry-outlook/agriculture/palm-oil/io/oil-palm-industry-2022-2024 (accessed Aug 4, 2023).

(19) Sukiran, M. A.; Chin, C. M.; Bakar, N. K. A. Bio-oils from pyrolysis of oil palm empty fruit bunches. *Am. J. Appl. Sci.* **2009**, *6*, 869−875.

(20) Salema, A. A.; Ani, F. N. Pyrolysis of oil palm empty fruit bunch biomass pellets using multimode microwave irradiation. *Bioresour. Technol.* **2012**, *125*, 102−107.

(21) Sembiring, K. C.; Rinaldi, N.; Simanungkalit, S. P. Bio-oil from fast pyrolysis of empty fruit bunch at various temperature. *Energy Procedia* **2015**, *65*, 162−169.

(22) Salema, A. A.; Ani, F. N. Microwave-assisted pyrolysis of oil palm shell biomass using an overhead stirrer. *J. Anal. Appl. Pyrolysis* **2012**, *96*, 162−172.

(23) Abnisa, F.; Daud, W. W.; Husin, W. N. W.; Sahu, J. N. Utilization possibilities of palm shell as a source of biomass energy in Malaysia by producing bio-oil in pyrolysis process. *Biomass Bioenergy* **2011**, *35*, 1863−1872.

(24) Mushtaq, F.; Abdullah, T. A. T.; Mat, R.; Ani, F. N. Optimization and characterization of bio-oil produced by microwave assisted pyrolysis of oil palm shell waste biomass with microwave absorber. *Bioresour. Technol.* **2015**, *190*, 442−450.

(25) Leng, L.; Li, H.; Yuan, X.; Zhou, W.; Huang, H. Bio-oil upgrading by emulsification/microemulsification: A review. *Energy* **2018**, *161*, 214−232.

(26) Lu, Q.; Li, W. Z.; Zhu, X. F. Overview of fuel properties of biomass fast pyrolysis oils. *Energy Convers. Manage.* **2009**, *50*, 1376−1383.

(27) Fu, P.; Bai, X.; Yi, W.; Li, Z.; Li, Y.; Wang, L. Assessment on performance, combustion and emission characteristics of diesel engine fuelled with corn stalk pyrolysis bio-oil/diesel emulsions with $Ce_{0.7}Zr_{0.3}O_2$ nanoadditive. *Fuel Process. Technol.* **2017**, *167*, 474−483.

(28) Irfan, M.; Ghalib, S. A.; Waqas, S.; Khan, J. A.; Rahman, S.; Faraj Mursal, S. N.; Ghanim, A. A. J. Response Surface Methodology for the synthesis and characterization of bio-oil extracted from biomass waste and upgradation using the rice husk ash catalyst. *ACS Omega* **2023**, *8*, 17869−17879.

(29) Ikura, M.; Stanciulescu, M.; Hogan, E. Emulsification of pyrolysis derived bio-oil in diesel fuel. *Biomass Bioenergy* **2003**, *24*, 221−232.

(30) Chiaramonti, D.; Oasmaa, A.; Solantausta, Y. Power generation using fast pyrolysis liquids from biomass. *Renewable Sustainable Energy Rev.* **2007**, *11*, 1056−1086.

(31) Lin, B. J.; Chen, W. H.; Budzianowski, W. M.; Hsieh, C. T.; Lin, P. H. Emulsification analysis of bio-oil and diesel under various combinations of emulsifiers. *Appl. Energy* **2016**, *178*, 746−757.

https://doi.org/10.1021/acsomega.3c05007
ACS Omega 2023, 8, 44586−44600

(32) Martin, J. A.; Mullen, C. A.; Boateng, A. A. Maximizing the stability of pyrolysis oil/diesel fuel emulsions. *Energy Fuels* **2014**, *28*, 5918−5929.
(33) Paramasivam, B.; Kasimani, R.; Rajamohan, S. Characterization of pyrolysis bio-oil derived from intermediate pyrolysis of Aegle marmelos de-oiled cake: study on performance and emission characteristics of CI engine fueled with Aegle marmelos pyrolysis oil-blends. *Environ. Sci. Pollut. Res.* **2018**, *25*, 33806−33819.
(34) Sukumar, V.; Manieniyan, V.; Sivaprakasam, S. Experimental studies on DI diesel engine fueled in sweet lime pyrolysis oil with biodiesel. *Int. J. Appl. Eng. Res.* **2019**, *14*, 1145−1150.
(35) Abnisa, F.; Arami-Niya, A.; Daud, W. M. A. W.; Sahu, J. N. Characterization of bio-oil and bio-char from pyrolysis of palm oil wastes. *BioEnergy Res.* **2013**, *6*, 830−840.
(36) Abnisa, F.; Wan Daud, W.; Sahu, J. N. Optimization and characterization studies on bio-oil production from palm shell by pyrolysis using response surface methodology. *Biomass Bioenergy* **2011**, *35*, 3604−3616.
(37) Somnuk, K.; Niseng, S.; Prateepchaikul, G. Optimization of high free fatty acid reduction in mixed crude palm oils using circulation process through static mixer reactor and pilot-scale of two-step process. *Energy Convers. Manage.* **2014**, *80*, 374−381.
(38) Ministry of energy. Determine the characteristics and quality of diesel fuel Home Page. http://elaw.doeb.go.th/document_doeb/TH/699TH_0001.pdf (accessed June 2, 2023).
(39) Oo, Y. M.; Thawornprasert, J.; Intaprom, N.; Rodniem, K.; Somnuk, K. Diesel-biodiesel-water fuel nanoemulsions for direct injection and indirect injection diesel engines: performance and emission characteristics. *ACS Omega* **2022**, *7*, 34951−34965.
(40) Gautam, R.; Kumar, S. Performance and combustion analysis of diesel and tallow biodiesel in CI engine. *Energy Rep.* **2020**, *6*, 2785−2793.
(41) Gautam, R.; Kumar, N. Comparative study of performance and emission characteristics of Jatropha alkyl ester/butanol/diesel blends in a small capacity CI engine. *Biofuels* **2015**, *6*, 179−190.
(42) Yuan, X.; Ding, X.; Leng, L.; Li, H.; Shao, J.; Qian, Y.; Huang, H.; Chen, X.; Zeng, G. Applications of bio-oil-based emulsions in a DI diesel engine: The effects of bio-oil compositions on engine performance and emissions. *Energy* **2018**, *154*, 110−118.
(43) Rizwanul Fattah, I.; Masjuki, H. H.; Kalam, M. A.; Mofijur, M.; Abedin, M. J. Effect of antioxidant on the performance and emission characteristics of a diesel engine fueled with palm biodiesel blends. *Energy Convers. Manage.* **2014**, *79*, 265−272.
(44) Mofijur, M.; Masjuki, H. H.; Kalam, M. A.; Atabani, A. E.; Fattah, I. R.; Mobarak, H. M. Comparative evaluation of performance and emission characteristics of Moringa oleifera and palm oil based biodiesel in a diesel engine. *Ind. Crops Prod.* **2014**, *53*, 78−84.
(45) Tan, Y. H.; Abdullah, M. O.; Nolasco-Hipolito, C.; Zauzi, N. S. A.; Abdullah, G. W. Engine performance and emissions characteristics of a diesel engine fueled with diesel-biodiesel-bioethanol emulsions. *Energy Convers. Manage.* **2017**, *132*, 54−64.
(46) Midhun Prasad, K.; Murugavelh, S. Experimental investigation and kinetics of tomato peel pyrolysis: Performance, combustion and emission characteristics of bio-oil blends in diesel engine. *J. Cleaner Prod.* **2020**, *254*, 120115.
(47) Subramanian, S.; Ramalingam, S.; Subramanian, A. An alternative fuel to CI engine: delonix regia seed through biochemical and solar-assisted thermal cracking process. *Int. J. Environ. Sci. Technol.* **2023**, *20*, 4017−4030.
(48) Mariappan, M.; Panithasan, M. S.; Venkadesan, G. Pyrolysis plastic oil production and optimisation followed by maximum possible replacement of diesel with bio-oil/methanol blends in a CRDI engine. *J. Cleaner Prod.* **2021**, *312*, 127687.
(49) Yadav, A. K.; Khan, O.; Khan, M. E. Utilization of high FFA landfill waste (leachates) as a feedstock for sustainable biodiesel production: its characterization and engine performance evaluation. *Environ. Sci. Pollut. Res.* **2018**, *25*, 32312−32320.
(50) Baranitharan, P.; Ramesh, K.; Sakthivel, R. Analytical characterization of the Aegle marmelos pyrolysis products and investigation on the suitability of bio-oil as a third generation bio-fuel for CI engine. *Environ. Prog. Sustainable Energy* **2019**, *38*, 13116.
(51) Ağbulut, Ü.; Sarıdemir, S.; Albayrak, S. Experimental investigation of combustion, performance and emission characteristics of a diesel engine fuelled with diesel-biodiesel-alcohol blends. *J. Braz. Soc. Mech. Sci. Eng.* **2019**, *41*, 389.
(52) Elkelawy, M.; Alm-Eldin Bastawissi, H.; El Shenawy, E.; Taha, M.; Panchal, H.; Sadasivuni, K. K. Study of performance, combustion, and emissions parameters of DI-diesel engine fueled with algae biodiesel/diesel/n-pentane blends. *Energy Convers. Manage.: X* **2021**, *10*, 100058.
(53) Elkelawy, M.; Kabeel, A. E.; El Shenawy, E.; Panchal, H.; Elbanna, A.; Bastawissi, H. A. E.; Sadasivuni, K. K. Experimental investigation on the influences of acetone organic compound additives into the diesel/biodiesel mixture in CI engine. *Sustain. Energy Technol. Assess.* **2020**, *37*, 100614.
(54) Peng, D. X. Exhaust emission characteristics of various types of biofuels. *Adv. Mech. Eng.* **2015**, *7*, 168781401559303.
(55) Gumus, M.; Sayin, C.; Canakci, M. The impact of fuel injection pressure on the exhaust emissions of a direct injection diesel engine fueled with biodiesel-diesel fuel blends. *Fuel* **2012**, *95*, 486−494.
(56) Pradhan, D.; Bendu, H.; Singh, R. K.; Murugan, S. Mahua seed pyrolysis oil blends as an alternative fuel for light-duty diesel engines. *Energy* **2017**, *118*, 600−612.
(57) Alptekin, E. Emission, injection and combustion characteristics of biodiesel and oxygenated fuel blends in a common rail diesel engine. *Energy* **2017**, *119*, 44−52.
(58) Abed, K. A.; Gad, M. S.; El Morsi, A.; Sayed, M. M.; Elyazeed, S. A. Effect of biodiesel fuels on diesel engine emissions. *Egypt. J. Pet.* **2019**, *28*, 183−188.
(59) Rajamohan, S.; Kasimani, R. Studies on the effects of storage stability of bio-oil obtained from pyrolysis of Calophyllum inophyllum deoiled seed cake on the performance and emission characteristics of a direct-injection diesel engine. *Environ. Sci. Pollut. Res.* **2018**, *25*, 17749−17767.
(60) El-Baz, F. K.; Gad, M. S.; Abdo, S. M.; Abed, K. A.; Matter, I. A. Performance and exhaust emissions of a diesel engine burning algal biodiesel blends. *Fuel* **2016**, *16*, 151−158.
(61) Mohapatra, S. S.; Rath, M. K.; Singh, R. K.; Murugan, S. Performance and emission analysis of co-pyrolytic oil obtained from sugarcane bagasse and polystyrene in a CI engine. *Fuel* **2021**, *298*, 120813.
(62) Rajamohan, S.; Kasimani, R. Analytical characterization of products obtained from slow pyrolysis of Calophyllum inophyllum seed cake: study on performance and emission characteristics of direct injection diesel engine fuelled with bio-oil blends. *Environ. Sci. Pollut. Res.* **2018**, *25*, 9523−9538.
(63) Shrivastava, P.; Verma, T. N.; Pugazhendhi, A. An experimental evaluation of engine performance and emisssion characteristics of CI engine operated with Roselle and Karanja biodiesel. *Fuel* **2019**, *254*, 115652.
(64) Janarthanam, H.; Kachupalli, S. R. S. R.; Jayapalan, S. K.; Subbiah, G.; Mani, P.; Velkumar, M.; Adithya, S. S. Emission and performance analysis of thermochemical conversion of bio-oil using waste animal fat. *AIP Conf. Proc.* **2020**, *2311*, 020020.
(65) Geng, P.; Mao, H.; Zhang, Y.; Wei, L.; You, K.; Ju, J.; Chen, T. Combustion characteristics and NO_x emissions of a waste cooking oil biodiesel blend in a marine auxiliary diesel engine. *Appl. Therm. Eng.* **2017**, *115*, 947−954.
(66) Asokan, M. A.; Senthur Prabu, S.; Bade, P. K. K.; Nekkanti, V. M.; Gutta, S. S. G. Performance, combustion and emission characteristics of juliflora biodiesel fuelled DI diesel engine. *Energy* **2019**, *173*, 883−892.
(67) Al-Dawody, M. F.; Bhatti, S. K. Experimental and computational investigations for combustion, performance and emission parameters of a diesel engine fueled with soybean biodiesel-diesel blends. *Energy Procedia* **2014**, *52*, 421−430.
(68) Silitonga, A. S.; Masjuki, H. H.; Ong, H. C.; Sebayang, A. H.; Dharma, S.; Kusumo, F.; Siswantoro, J.; Milano, J.; Daud, K.; Mahlia,

https://doi.org/10.1021/acsomega.3c05007
ACS Omega 2023, 8, 44586−44600

T. M. I.; Chen, W. H.; Sugiyanto, B. Evaluation of the engine performance and exhaust emissions of biodiesel-bioethanol-diesel blends using kernel-based extreme learning machine. *Energy* **2018**, *159*, 1075−1087.
(69) Mulimani, H.; Navindgi, M. C. An experimental investigation of DI diesel engine fuelled with emulsions of Mahua bio-oil. *Indian J. Sci. Res.* **2017**, *6*, 1781−1785.

https://doi.org/10.1021/acsomega.3c05007
ACS Omega 2023, 8, 44586−44600